Dynamic Resilience of Interdependent Freight Infrastructure and Multimodal Logistics Facilities

Davis C. Loose, *Member, IEEE*, Megan C. Marcellin*, Member, IEEE*, Megan E. Gunn, *Member, IEEE,* Matthew C. Gunn, *Member, IEEE,* Femi Popoola, Karen R. Jackson, Eric Jehu, Igor Linkov*,* and James H. Lambert, *Fellow, IEEE*

***Abstract*— Freight networks consist of interdependent infrastructure sectors whose failures can cascade across manufacturers, carriers, and logistics operators. Predictable and secure freight operations require analytical methods that represent both the infrastructure sectors enabling regional commerce and the physical assets that constitute them. This study introduces a dynamic capacity propagation model on a hybrid sector-asset network to simulate how disruptions cascade through interdependent infrastructure over time. The model is a network graph linking sixteen critical infrastructure sectors with thirty-six regional assets, establishes baseline system structure using eigenvector centrality, and applies time-stepped capacity dynamics to quantify how disruptions reorder the importance of network components. A pull-based buffer mechanism represents how multimodal logistics parks (MMLPs) inject supplemental capacity into sectors during disruptions. Resilience is assessed as the disruption of system order, measured by the Spearman rank correlation between baseline and disrupted centrality rankings. The model is tested on an industrial region of the mid-Atlantic United States across six disruptive scenarios. Results include that the type of disruption influences both the magnitude and trajectory of system reordering, and that MMLPs improve system resilience. The model is thus a significant new capability for designing supply chains and distributed manufacturing that involve rail, road, maritime, aviation, and other freight modes.**

***Index Terms*—** Systems engineering, risk management, supply chains, network analysis, stress testing, performance evaluation

I. Introduction

The operations of firms, carriers, and regional supply chains face growing exposure to uncertain and compounding risks [1]. These risks are amplified by interdependencies linking infrastructure sectors, logistics operators, manufacturers, regulatory bodies, and other actors. A failure in one or more of these areas can propagate through these interdependencies and impair performance in other, seemingly unrelated sectors [2]. The 2026 winter storms in North America produced cascading impacts across supply networks, with projected global economic losses exceeding $105 billion worldwide [3].

Interdependencies span physical, cyber, geographic, and logical dimensions, linking systems through shared resources, data flows, co-location, and operational policies [4]. Freight systems depend on sectors such as energy, transportation, and communications that are themselves interdependent [5]. Stakeholders operating across these interdependencies have different objectives, risk tolerances, and planning horizons, making coordinated resilience investment difficult [6]. Regions address these challenges through shared infrastructure investment, cross-sector contingency planning, and operational strategies that reduce exposure to cascading failures [7]. For freight systems, one emerging approach is the development of multimodal logistics parks (MMLPs).

MMLPs are specialized infrastructure hubs that consolidate road and rail freight handling, advanced warehousing, cold-chain services, intermodal exchange, and related operations at a single facility [8]. These capabilities position MMLPs at the intersection of multiple critical infrastructure sectors, including healthcare, manufacturing, defense, energy, and agriculture, thereby supporting regional stability and resilience [9].

Prior work established a graph-based framework for assessing infrastructure resilience through the disruption of system order, in which centrality-based rankings of critical infrastructure sectors are compared before and after disruptive events [10]. A further extension of this introduced a hybrid sector-asset network linking abstract sector interdependencies with physical asset inventories, enabling analysis at both the system-of-systems and operational scales [11]. Other work has examined how disruptions to production capacity in one part of an interdependent sociotechnical network produce proportional reductions in others [12]. However, these models have not been applied to hybrid sector-asset freight networks or used to evaluate the resilience contribution of specific infrastructure investments such as MMLPs. Methods for assessing how

This effort was supported in part by the Commonwealth Center for Advanced Logistics Systems (CCALS), the Virginia Economic Development Partnership (VEDP), US National Science Foundation Center for Hardware and Embedded Systems Security and Trust (NSF CHEST), the Virginia Department of Transportation (VDOT), and the US Army Corps of Engineers (USACE), (Corresponding author: Davis C. Loose)

Davis C. Loose is with the University of Virginia Department of Systems and Information Engineering, Charlottesville, VA 22904 USA (email: dcl6d@virgnina.edu)

Megan C. Marcellin is with the University of Virginia Department of Electrical and Computer Engineering, Charlottesville, VA 22904 USA (email: mcm5ft@virginia.edu)

Megan E. Gunn is with the University of Virginia Department of Systems and Information Engineering, Charlottesville, VA 22904 USA (email: meg9hq@virginia.edu)

Matthew C. Gunn is with the University of Virginia Department of Systems and Information Engineering, Charlottesville, VA 22904 USA (email: mcg3er@virginia.edu)

Femi Popoola is with the Virginia Economic Development Partnership, Richmond, VA 23219 (email: fpopoola@vedp.org)

Karen R. Jackson is with the Commonwealth Center for Advanced Logistics Systems, Petersburg, VA 23805 (email: karenrjackson2010@gmail.com)

Eric Jehu is with the Virginia Economic Development Partnership, Richmond, VA 23219 (email: ejehu@vedp.org)

Igor Linkov is with the U.S. Army Corps of Engineers: Engineer Research and Development Center, Concord, MA 01742 USA (email: Igor.Linkov@usace.army.mil)

James H. Lambert is the Director of the University of Virginia Center for Risk Management of Engineering Systems, Charlottesville, VA 22904 USA (email: lambert@virginia.edu)

disruptions propagate through interdependent regional infrastructure, and how the resulting structural reordering varies across disruption types and network configurations are limited. The method advanced in this study addresses this need by modeling how disruptions influence system order in adaptive representations of regional infrastructure.

Addressing this limitation would provide regional planners, logistics operators, and infrastructure investors with a quantitative basis for evaluating how network structure influences regional resilience under disruption. The contributions of this study are: (1) advancing the hybrid sector-asset network of regional logistics to incorporate dynamic disruption propagation over time, (2) introducing a buffer mechanism for MMLPs that allows them to supplement performance of degraded sectors, and (3) developing a disruption model that reduces node performance rather than removing nodes from the network, capturing gradual degradation and recovery. The method provides a basis for evaluating how structural design choices in interdependent regional infrastructure affect resilience under different disruptive scenarios.

II. Background

The Cybersecurity and Infrastructure Security Agency (CISA) organizes critical infrastructure into sixteen sectors, spanning Energy, Transportation Systems, Communications, Healthcare, and other domains essential to national security and economic stability [13]. These sectors are interdependent through physical, cyber, geographic, logical, and hierarchical linkages such that a failure in one sector can impact performance in another. Network-based representations model these interdependencies as graphs, where sectors are nodes and edges represent functional or operational relationships [2],[14]. Centrality metrics identify which sectors are most structurally important and which are vulnerable to different types of disruption [15],[16]. Prior assessments have used these representations to evaluate how node removals and capacity reductions alter the structure of infrastructure networks [9], [10].

Freight systems face challenges in the interdependent infrastructure context. Freight operations span multiple sectors simultaneously, requiring services that support the production and movement of goods through a region [17]. One approach to managing cross-sector dependencies is the development of MMLPs, which consolidate freight handling across a variety of modalities and operational requirements at a single facility [18]. MMLPs offer cross docking, less-than-truckload break-bulk, temperature-controlled storage and distribution, customs processing, advanced warehousing and management, and security features. These capabilities position MMLPs at the center of multiple infrastructure sectors, creating a structural role in regional logistics networks beyond freight handling.

Interdependent infrastructure resilience has been studied using network models, scenario-based stress testing, simulation, and dependency mapping [19]-[21]. These methods assess how disruptions propagate across infrastructure through shared resources, service dependencies, and operational relationships. Network-based approaches are well suited to interdependent infrastructure because they represent sectors and assets as connected nodes and edges, enabling analysis of cascading failures, vulnerable dependencies, and structural influence of system components [22 Prior work has applied these methods to assess resilience under node removals, link failures, and capacity degradation, showing that disruption outcomes depend on both the directly affected components and the structure of the interdependencies through which disruptions spread [2], [9]–[11]. This frames resilience as a system-level property shaped by component performance and network structure.

Network-based resilience assessments have emphasized the structural importance of infrastructure components and the extent to which disruption alters their relative roles in the system [23]. Centrality metrics quantify structural importance by identifying the sectors or assets that are most influential within a pattern of interdependencies [15], [16]. Prior work has extended this perspective by defining resilience in terms of preservation of system order, measured as the stability of the ranked order of system components [24]. In this framing, Spearman rank correlation provides a useful measure of disruption because it captures how the orders of sectors and assets change under stress rather than only the magnitude of capacity loss [25]. Dynamic resilience emphasizes how systems change over time under disruption rather than only whether they fail [26]. Resilience curves represent this this temporal behavior through phases such as prepare, absorb, respond, and recover, showing depth of performance loss and the trajectory of recovery. In infrastructure systems, this perspective is important because two disruptions may produce similar losses in operational capacity while differing in how impacts spread, how long instability persists, and how recovery occurs.

This study examines a mid-Atlantic industrial region in the United States defined by multimodal connectivity, including two major north-south freight corridors, east-west connectors, extensive highway coverage, rail access, and links to deepwater container terminals with direct truck and rail service [27], [28]. This geography supports high freight throughput and positions the region for continued logistics growth through access to major domestic consumer markets. The region also contains a dense base of specialized manufacturers, including pharmaceutical, defense, and electronics producers, whose operations depend on reliable cross-sector infrastructure. These characteristics make the region a useful setting for evaluating interdependent infrastructure resilience.

III. Overview of Regional Infrastructure Network

Critical infrastructure resilience analysis requires modeling the assets and interdependencies that constitute regional productive capacity. This section develops a hybrid sector-asset network for a regional logistics context, in which sector-level interdependencies are associated with specific facilities, manufacturers, and logistics infrastructure within a bounded geographic region.

Fig. 1 describes the *sector* layer which consists of the sixteen CISA critical infrastructure sectors, represented as nodes in a directed graph. Each sector is denoted $s \in S$. Edges between sectors represent documented cross-sector interdependencies, with all pairwise connections initialized at a uniform baseline weight. Directional asymmetries between sector pairs are supported by the model, but are not introduced here given limited empirical justification.

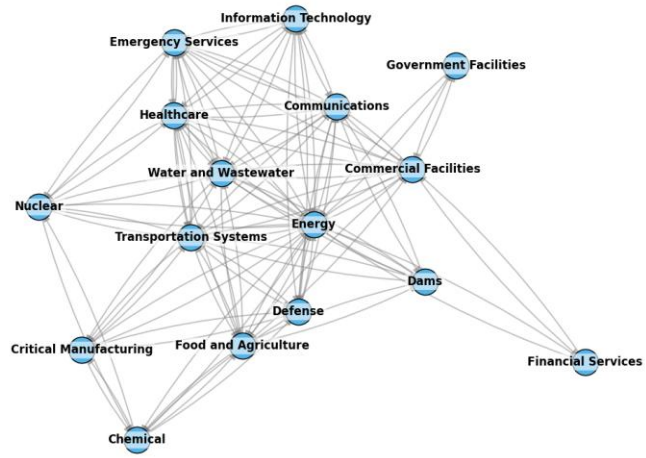

Fig. 1. Network representation of interdependencies among 16 CISA critical infrastructure sectors. Nodes represent sectors and edges represent functional, physical, or informational links.

Fig. 2 shows the asset layer, consisting of thirty-six facilities and organizations selected based on physical presence or influence in the study region, sectoral significance, and data availability. Each asset is denoted $a \in A$. Nodes are colored by geographic and functional role; blue nodes represent manufacturers located within the study region, pink nodes represent manufacturers located outside the region whose operations influence regional infrastructure capacity, green nodes represent external warehousing and logistics facilities representing different distribution modes, and yellow nodes represent the two MMLPs, which serve as the primary connective hubs of the regional asset network. The assets are connected by edges representing physical freight corridors such as rail or road. Assets are grouped into seventeen functional classes, including pharmaceutical manufacturers, agricultural producers, chemical producers, and intermodal logistics facilities, each representing a distinct source of productive capacity in the regional logistics network.

Asset classes are mapped to sectors in two directions, reflecting both their contributions to regional sector capacity and their dependence on sector-level infrastructure. Provision relationships reflect the role each asset class plays within one or more sectors, drawing on CISA sector profiles and subject matter expert assessment [10]. Dependency relationships reflect the sector-level inputs each asset class requires to operate at full capacity. All assets depend on the Energy, Transportation Systems, and Communications sectors, while other sector-specific dependencies, such as Water and Wastewater Systems and Food and Agriculture, are assigned individually. Table I defines the reciprocal mapping between asset classes and sectors, with each entry representing the edge weight for a class-sector relationship. For each asset class, the $A \rightarrow S$ weights sum to 1.0, such that each weight denotes the share of the productive contribution of that class assigned to a given sector. The corresponding $S \rightarrow A$ edges represent the mirrored sectoral dependencies that sustain operation of that asset class.

The hybrid graph $H = (V, E)$ provides the baseline structure for the model in subsequent sections, where disruptive scenarios reduce operational capacity for assets and sectors. Sector-to-sector (S→S) edges are formed by the directed sector graph, asset-to-asset (A→A) by the regional logistics network, and the asset-to-sector (A→S) and sector-to-asset (S→A) edges by the functional contributions of each asset class to regional capacity and the sector-level inputs each asset class requires to operate. MMLPs are structurally distinct assets in this network. Warehouse assets represent storage facilities outside the target region with limited operational scope, providing capacity only to Transportation Systems and Commercial Facilities. By contrast, MMLPs provide cross-docking, less-than-truckload break-bulk, temperature-controlled distribution, and intermodal transfer capabilities that generic warehouses do not [8]. This allows MMLPs to serve as intermediaries across a broad set of sectors including Healthcare, Food and Agriculture, and Critical Manufacturing. This role motivates the buffering mechanism developed in the following section, in which MMLPs act as regional resilience infrastructure capable of partially restoring degraded sector operational capacity.

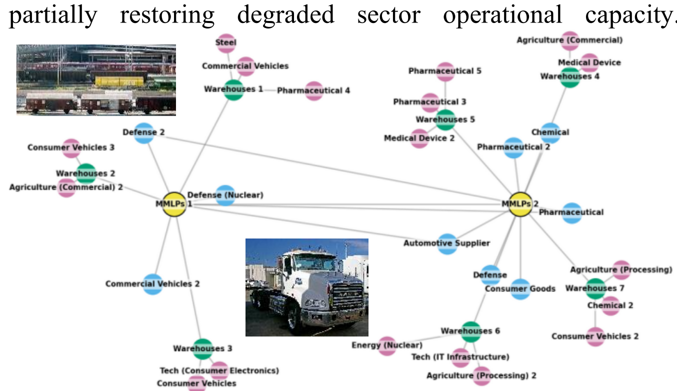

Fig. 2. Asset-level network of the mid-Atlantic industrial region with two multimodal logistics parks [10],[29],[30]. Freight travels between assets by road, rail, and other vectors.

IV. Technical Approach

The preceding section established the structure of the hybrid sector-asset network. This section describes the modeling choices governing how operational capacity propagates through the network under disruption. The objective is to assess regional infrastructure resilience as the disruption of system order, where system order is defined as the ranking of hybrid sector-asset network components by eigenvector centrality, reflecting their structural importance to regional interdependencies. Eigenvector centrality is selected because it captures recursive interdependency, where the importance of a node depends not only on its own connections, but on the importance of its neighbors [2], [11]. This provides a measure of structural sensitivity to disruption. Components that shift in rank under disruption are those whose structural importance is most affected the disruption in question. The resulting change in total rank order during disruption provides system-level measure of disruption.

Nodes are ranked by eigenvector centrality to establish the baseline state of the network. Each node is assigned an operational capacity $c_i(t)$ initialized to 1.0 at $t = 0$. Disruptions degrade the operational capacity of nodes over a defined time window. During disruption, nodes lose operational capacity over a defined time window through a propagation mechanism that transmits pressure along weighted edges. Reduced node capacity scales the effective edge weight $w_{ij}(t)$, which in turn alters the eigenvector centrality rankings that define system order.

TABLE I. EDGES AND WEIGHTS BETWEEN CRITICAL INFRASTRUCTURE SECTORS AND ASSET CLASSES

Asset Class	Trans. Sys.	Energy	Comms.	IT	Crit. Mfg.	Nucl.	Fin. Svc.	Water	Comm. Fac.	Health.	Food & Ag.	Defense	Gov. Fac.	Emerg. Svc.	Chem.	Dams
MMLPs	0.23	0.05	0.10	0.10	0.08	–	–	–	0.15	0.13	0.18	–	–	–	–	–
Warehouses	0.58	–	–	–	–	–	–	–	0.42	–	–	–	–	–	–	–
Ag. (Commercial)	–	–	–	–	–	–	–	–	0.25	–	0.75	–	–	–	–	–
Ag. (Processing)	–	–	–	–	–	–	–	–	0.46	–	0.54	–	–	–	–	–
Energy (Nuclear)	–	0.66	–	–	0.14	0.21	–	–	–	–	–	–	–	–	–	–
Defense	–	–	–	–	–	–	–	–	–	–	–	0.75	0.25	–	–	–
Defense (Nuclear)	–	0.25	–	–	–	0.20	–	–	–	–	–	0.40	0.15	–	–	–
Commercial Vehicles	0.69	–	–	–	0.31	–	–	–	–	–	–	–	–	–	–	–
Consumer Vehicles	0.46	–	–	–	0.23	–	–	–	0.31	–	–	–	–	–	–	–
Auto. Supplier	0.27	–	–	–	0.53	–	–	–	–	–	–	–	–	0.20	–	–
Chemical	–	–	–	–	0.25	0.15	–	–	–	–	0.15	–	–	–	0.45	–
Pharmaceutical	–	–	–	–	–	–	–	–	–	0.83	–	–	–	–	0.17	–
Medical Device	–	–	–	–	–	–	–	0.20	–	0.60	–	–	0.20	–	–	–
Steel	0.31	0.13	–	–	0.56	–	–	–	–	–	–	–	–	–	–	–
Tech (IT Infra.)	–	–	0.35	0.45	–	–	0.20	–	–	–	–	–	–	–	–	–
Tech (Cons. Elec.)	–	–	–	–	0.36	–	–	–	0.64	–	–	–	–	–	–	–
Consumer Goods	0.25	–	–	–	–	–	–	–	0.75	–	–	–	–	–	–	–

A recovery term restores operational capacity toward 1.0 at each timestep in proportion to the current deficit. In the MMLP configuration, a pull-based buffer mechanism allows degraded sectors to draw supplemental capacity from MMLP nodes during the disruption window, reducing the impact of disruption. At each timestep, eigenvector centrality is recomputed on the capacity-weighted graph and compared to the baseline ranking using Spearman's rank correlation coefficient ρ [25]. The primary disruptiveness metric is the maximum deviation from baseline order, $D = 1 - min_t\, \rho$. Each scenario is run with and without the MMLP buffer, and the resulting difference ΔD isolates the resilience contribution of the MMLP.

Edge weights in the hybrid graph vary by edge type and direction. S→S edges are initialized at a uniform baseline weight $w_{ij}^{\text{baseline}} = 1.0$, consistent with previous iterations of the framework [2]. A→A edges are undirected and uniformly weighted at 1.0, representing physical connectivity between facilities without differentiating by mode or capacity. Each asset class distributes its full operational capacity across the sectors it supports. For each asset class, the A→S weights w_{ij}^{norm} sum to 1.0, so that each weight represents the share of operational capacity given to a sector. For example, he pharmaceutical class, distributes across Healthcare and Chemical, while the MMLP class distributes across eight sectors. All assets within the same class share the same weight vector. This structure allows subject matter experts to assess relative sectoral contributions within a single asset class. S→A edges enforce interdependency by mirroring the weight of the corresponding A→S edge as $w_{ij}^{\text{m}} = w_{ji}^{\text{norm}}$, $(i,j) \in E_{SA}$. This creates a reciprocal relationship between assets and sectors, assets depend on sector-level services to operate, while sectors depend on the assets that constitute them. The Energy, Transportation Systems, and Communications sectors maintain S→A edges to all asset nodes regardless of whether a corresponding A→S edge exists, with a default weight of $w_{ij}^{\text{baseline}} = 1.0$. This reflects the assumption that all assets require power, transportation access, and communications connectivity to function, even when those assets do not contribute directly to those sectors.

Each node $i \in V$ carries an operational capacity $c_i(t)$ bounded between a floor $\underline{c}_i$ and ceiling $\bar{c}_i$. All nodes are initialized $c_i(0) = 1.0$, and the ceiling is fixed at 1.0 for all nodes. Asset floors are uniform at 0.2 while sector floors vary and are derived from the number of assets n_i that provide to each sector. All capacity parameters are tunable, allowing configurations that range from negligible disruption to near-total system collapse. The floor values used in this study are not empirically calibrated. The objective of the model is to examine system-level resilience and interdependent cascade behavior rather than predict specific operational outcomes.

With capacities initialized, the baseline ranking of all nodes is established by eigenvector centrality on the full network. The eigenvector centrality x_i of node i is:

$$x_i = \frac{1}{\lambda} \sum_{j \neq i} w_{ij}\, x_j \tag{1}$$

where λ is the largest eigenvalue of the weighted adjacency matrix. At baseline, all capacities are 1.0 and edge weights equal their baseline values, defining the baseline system order.

At each timestep during a disruption nodes transmit downward pressure to neighboring nodes along the weighted edges. The pressure on a receiving node i is proportional to the baseline edge weight w_{ij}^{baseline}, the current capacity of the receiving node $c_i(t)$, and the capacity deficit $1 - c_j(t)$ of the transmitting node j. Two propagation rates govern the strength of this transmission; A→S and S→A edges use the propagation rate α. S→S edges use a weaker rate α_S, reflecting the assumption that inter-sector cascade rates are slower than between interdependent assets and sectors. Let N_i^{AS} be the set of predecessors of node i along A→S and S→A edges, and N_i^{S} be the set of predecessors along S→S edges. The pressure terms are defined as:

$$P_i^{AS}(t) = \frac{\alpha}{\left|N_i^{AS}\right|} \sum_{j \in N_i^{AS}} w_{ji}^{\text{baseline}}\, c_i(t) \left(1 - c_j(t)\right) \qquad (2a)$$

$$P_i^{S}(t) = \frac{\alpha_S}{\left|N_i^{S}\right|} \sum_{j \in N_i^{S}} w_{ji}^{\text{baseline}}\, c_i(t) \left(1 - c_j(t)\right) \qquad (2b)$$

Total pressure on each node is normalized by the number of incoming edges of each type, so nodes with many predecessors are not disproportionately degraded. A recovery term $R_{i(t)}$, governed by the recovery rate β restores operational capacity toward 1.0 at each timestep proportional to the current deficit.

$$R_{i(t)} = \beta\left(1 - c_{i(t)}\right) \qquad (3)$$

Node capacity is updated based on the state from the previous timestep. During the active disruption window, directly disrupted nodes may be held to the capacity floor $\underline{c_i}$ preventing the recovery term from reversing the imposed disruption. The reduced capacity of each node scales the weights of its incident edges at each timestep as:

$$w_{ij}(t) = w_{ij}^{\text{baseline}} c_i(t) c_j(t) \qquad (4)$$

where $w_{ij}(t)$ is the weight of the edge between nodes i and j. As edge weights change, the eigenvector centrality scores and rankings of nodes shift, causing a structural reordering of the system.

The disruption propagation mechanism described above transmits pressure from degraded assets towards the sectors they constitute. In turn, degraded sectors constrain the assets that depend on them. If the Healthcare sector degrades, pharmaceutical manufacturers that depend on it face reduced operational capacity reflecting changes in demand, workforce availability, regulatory uncertainty, and supply chain coordination. This ceiling is applied after the propagation update:

$$c_i(t+1) = \min\left(c_i(t+1), \min_{j \in N_i^{SA}}\left[w_{ji}^{\text{m}} c_j(t) + \left(1 - w_{ji}^{\text{m}}\right)\right]\right) \qquad (5)$$

That is, the asset takes the lower of two values: the capacity computed from propagation and recovery, or the capacity allowed by the most degraded sector it depends on. When the mirrored weight $w_{ji}^{\text{m}} = 1$, asset capacity cannot exceed sector capacity. When $w_{ji}^{\text{m}} = 0$, the sector imposes no constraint.

This study evaluates the resilience contribution of MMLPs by allowing them to inject supplemental capacity into sectors for which they have outgoing provision edges. This capability can be turned on or off without altering network structure. When inactive, MMLP nodes function as standard warehousing assets. When active, the buffer mechanism operates during disruption. Subsequent sections compare the two configurations to highilght the effect of MMLP buffering.

Degraded sectors draw from the MMLP buffer in proportion to their current deficit. This injection reflects the ability of MMLPs to provide freight at the required handling unit, such as full truckload, pallet, or parcel, through intermodal sorting and consolidation. The injection into sector s at timestep t is:

$$\phi_s(t) = \sum_{m \in \mathcal{M}} c_m(t)\, w_{ms}^{\text{norm}} \left(1 - c_s(t)\right) \delta^t \kappa \qquad (6)$$

where $\mathcal{M}$ is the set of MMLP nodes, $c_{\text{m}}(t)$ is the current capacity of the MMLP, w_{ms}^{norm} is the normalized provision weight from MMLP m to sector s, $\left(1 - c_s(t)\right)$ is the sector deficit that drives the pull signal, δ is the buffer decay factor, and κ is the MMLP strength controlling injection magnitude. The MMLP injection is capped as $\phi_s^*(t) = \min\left(\phi_s(t), 1 - c_s(t)\right)$ so that sector capacity does not exceed 1.0. The buffer activates after a lag of τ timesteps following disruption onset, representing operational delay. The buffer stops injecting at the end of the disruption window or when the decay term falls below a minimum threshold (.01), whichever occurs first. The complete capacity update at each timestep combines pressure, recovery, and injection, subject to the operational bounds of the node as:

$$c_i(t+1) = c_i(t) - P_i^{AS}(t) - P_i^{S}(t) + R_i(t) + \phi_i^*(t) \qquad (7)$$
$$\text{subject to. } \underline{c_i} \le c_i(t+1) \le \overline{c}_i$$

That is, the new capacity equals the previous capacity minus downward pressure from degraded neighbors, plus autonomous recovery and any MMLP injection, bounded by the minimum and maximum capacities of the node.

TABLE II. DISRUPTIVE SCENARIOS USED TO ASSESS REGIONAL INFRASTRUCTURE RESILIENCE

Scenario	Type	Targeted Nodes	Analog
Cold Chain Disruption	Asset class (broad)	All Pharmaceutical assets (5)	Drug shortage, refrigeration failure
Steel and Auto Compound Shock	Multi-asset compound	Steel, Commercial Vehicle, and Consumer Vehicle assets (6)	Trade restrictions, cascading industrial shutdown
Nuclear Asset Stress	Asset class (shared sectors)	Energy (Nuclear) and Defense (Nuclear) assets (2)	Regulatory shutdown
Emergency Fleet Failure	Sector-asset hybrid	Emergency Services sector, Commercial Vehicle and Automotive Supplier assets (3)	Severe weather disabling emergency fleets and vehicle production
Communications Disruption	Sector-only (highly connected)	Communications sector (1)	Cyberattack, major carrier outage
Dam Failure	Sector-only (low connected)	Dams sector (1)	Flooding event, structural failure

Six disruption scenarios are used to evaluate regional logistics infrastructure resilience. Each scenario targets a subset of sectors and/or assets that experience capacity reductions from $t = 10$to $t = 20$. The set includes three asset-only disruptions, representing a full asset class, a multi-asset compound shock across classes, and a narrow group of assets with overlapping but not identical sector relationships. The remaining scenarios include one combined sector-asset disruption and two sector-only disruptions, one affecting a highly interconnected sector and one a weakly connected sector. Table II summarizes the six scenarios, their disruption types, and the targeted nodes.

Fig. 3 shows the response of selected sectors and assets under the Cold Chain Disruption scenario. In the sector-level panel, Healthcare and Public Health experiences the greatest operational capacity loss because it is most directly linked to the disrupted Pharmaceutical assets, while Chemical degrades more moderately and Food and Agriculture less so. In the asset-level panel, Pharmaceutical 1 is representative of the five disrupted assets, all of which are held at their floor values during the disruption window and recover afterward. Medical

Device 1 is not directly disrupted but still loses operational capacity through its dependency on the Healthcare sector. Solid and dashed lines denote the MMLP and non-MMLP configurations, respectively. The shaded regions show the disruption window and period of MMLP injection. The MMLP buffering is able to reduce the operational capacity loss in the Healthcare sector, which in turn reduces the capacity loss of the Medical Device 1 asset.

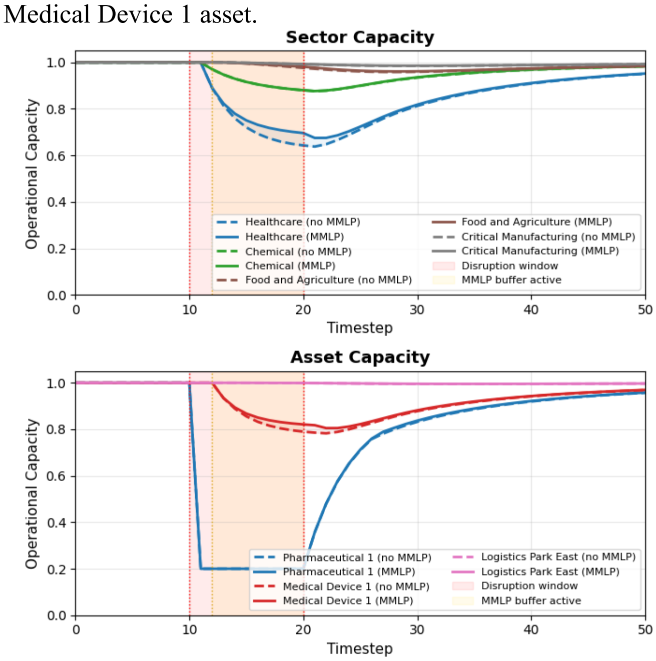

Fig. 3. Operational capacity trajectories for selected sectors and assets under the Cold Chain Disruption scenario.

The primary resilience metric in this study is the disruption of system order. At baseline, all nodes are ranked by eigenvector centrality. During disruption, reductions in node operational capacity alters edge weights and shifts those rankings. The degree of system order disruption is measured by Spearman's ρ between the baseline (non-disrupted) ranking and the disrupted ranking at each time step. The disruptiveness metric is the maximum departure from baseline over the full simulation.

$$D = 1 - \min_{t\in[0,T]} \rho\left(r^{\text{baseline}}, r(t)\right) \tag{8}$$

Values of D near zero indicate little disruption to system order, while larger values indicate greater structural reordering. Nodes pinned to their floor capacity during disruption are excluded from the Spearman calculation so that the metric reflects reordering in the rest of the system rather than the forced rank change of directly disrupted nodes. Each scenario is run with and without the MMLP buffer, and the resulting disruptiveness values are compared. Table III summarizes key terms and parameters used in this section.

V. Results

The following results apply the framework to the mid-Atlantic industrial region across the six disruptive scenarios. Fig. 4 shows the rank range for a representative subset of sectors and assets. All nodes are evaluated, but only selected examples are displayed. If a sector or asset is directly disrupted such that the scenario itself reduces it to its floor capacity, that forced rank change is excluded from the graph.

Table III. Model parameters, symbols, descriptions and base values

Symbol	Description	Value
S, A	Sector and asset node sets	16 sectors, 36 assets
$\underline{c}_i, \overline{c}_i$	Capacity limits	0.2 , 1.0
w_{ij}	Edge weight	1.0 (S→S, A→A); varies (A→S, S→A)
α, α_s	Propagation rates (cross-layer, sector-sector)	0.3, 0.05
β	Recovery rate	0.2
κ	MMLP buffer strength	0.5
δ	MMLP buffer decay factor	0.95
τ	MMLP activation lag	2 timesteps
T, T_d	Simulation length; disruption window	50; [10, 20]
D	Disruptiveness ($1 - \min \rho$)	Computed

The black diamonds show the baseline eigenvector centrality ranking, while the red and blue bars show the largest decrease and increase in rank experienced by each node across the six scenarios at the point of maximum disruption. The highest ranked nodes are primarily sectors, reflecting their dense interdependencies, and these sectors are generally stable under disruption. Notable exceptions include Healthcare, which falls substantially from its baseline position, and Nuclear and Critical Manufacturing, which show greater volatility across scenarios. Among assets, pharmaceutical manufacturers and the MMLPs are highly ranked but also sensitive to disruption, especially in the Cold Chain scenario, indicating that highly connected nodes can be both structurally important and vulnerable to reordering.

Fig. 5 tracks Spearman rank correlation over the full simulation for each scenario using all nodes. The six scenarios produce distinct disruption profiles, with the three asset-only scenarios showing steady degradation through the disruption window followed by recovery. In these cases, the MMLP configuration maintains higher ρ, reducing both peak disruption and the total departure from baseline. For example, in the Cold Chain Disruption scenario, disruptiveness declines from about 0.118 to 0.101. These results suggest that MMLPs reduce instability and improve recovery in asset-originated disruptions. The Emergency Fleet Failure and Communications Disruption produce the largest disruptions, with ρ falling to about 0.45 and 0.62, respectively. Both show a plateau during the disruption window, consistent with the "respond" phase of resilience curves [26]. The MMLP buffer provides less benefit in these cases because disruption originates at the sector layer and bypasses typical MMLP provisioning pathways. By contrast, Dam Failure produces little structural reordering because the Dams sector has few interdependencies and limited propagation pathways.

Fig. 6 summarizes disruptiveness scores across all six scenarios. The scenario ranking is consistent with the trajectory analysis, with Emergency Fleet Failure and Communications Disruption producing the greatest disruptiveness and Dam Failure the least. Among the asset-originated scenarios, Cold Chain Disruption is the most disruptive. Across the asset-originated scenarios, the MMLP has the greatest relative effect, suggesting that the buffer mechanism is most effective when disruption pathways pass through the asset layer.

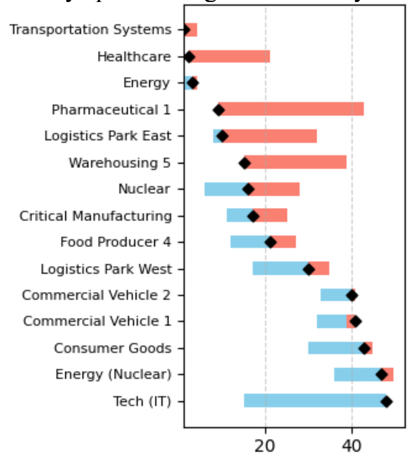

Fig. 4. Baseline ranking and disruption-induced rank ranges for selected sectors and assets.

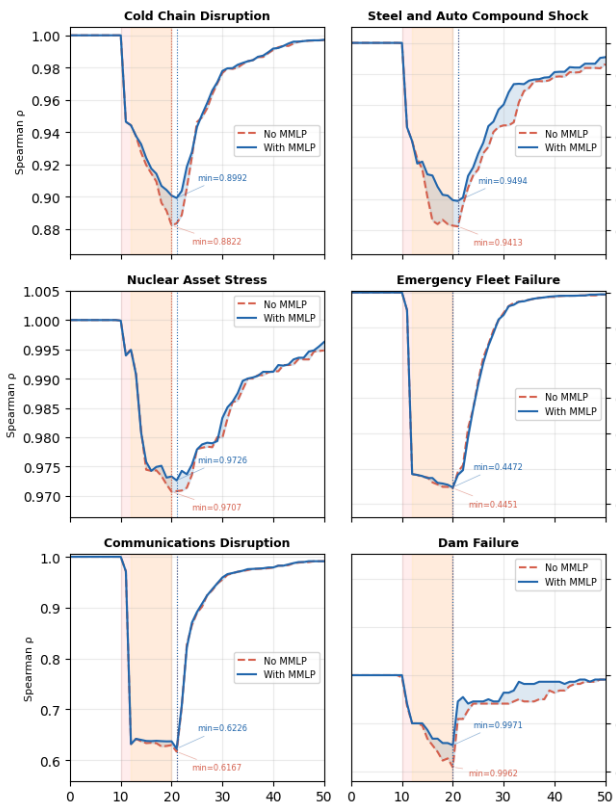

Fig. 5. Spearman rank correlation over fifty days for each disruptive scenario, comparing the MMLP (solid) and baseline (dashed) configurations for all nodes. The shaded regions denote the disruption window and period of active MMLP buffer injection.

Fig 7 isolates sector-level reordering by excluding changes in asset ranks, providing a perspective that may be more relevant for stakeholders focused on regional infrastructure stability than on facility-level disruption. The overall scenario ordering is similar to the full-network results, but two differences stand out. First, the MMLP buffer has a more pronounced effect in the sector-only analysis, suggesting that it stabilizes regional infrastructure even when individual asset rankings remain volatile. Second, the resilience profiles shift: asset-originated scenarios now show a plateau before recovery rather than the more continuous degradation seen in the full-network view, indicating that sector interdependencies can absorb and redistribute some asset-level shocks.

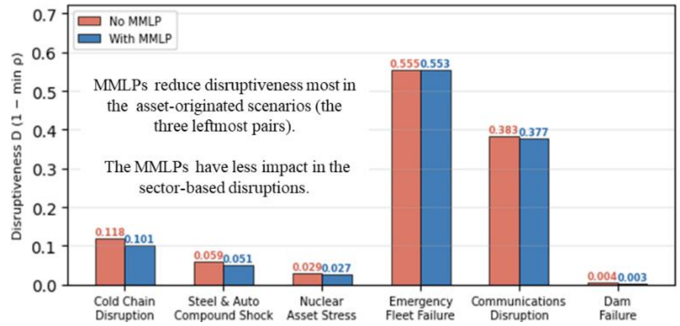

Fig. 6. Disruptiveness scores for six scenarios comparing baseline and MMLP configurations using all nodes in the hybrid graph.

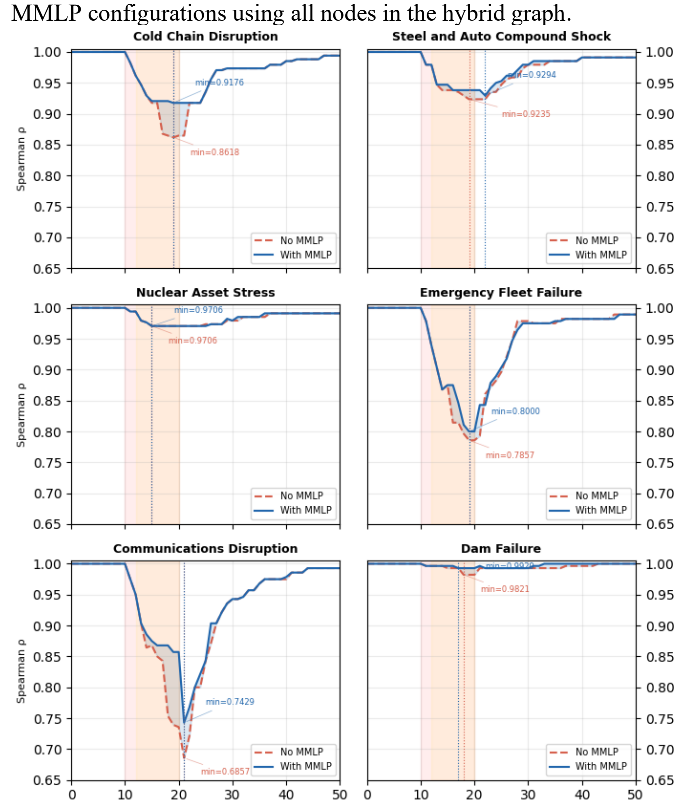

Fig. 7. Sector-only analysis of Spearman's rank correlation over fifty days of simulation.

V. Discussion and Conclusion

This study developed a dynamic capacity propagation model on a hybrid sector-asset network to assess how disruptions cascade through interdependent regional infrastructure over time. The model integrates sixteen critical infrastructure sectors with thirty-six assets representing regional logistics functions such as manufacturers, warehouses, and MMLPs. The edges of the graph denote interdependencies between sectors, assets, and the two layers. Nodes are ranked by eigenvector centrality to establish a baseline system order, and disruptions are quantified by the degree to which that order changes over time. The MMLPs provide can provide buffer capacity to infrastructure sectors during disruption. Six scenarios spanning four disruption typologies were applied to a mid-Atlantic industrial region, each run with and without the MMLP buffer to isolate its resilience contribution. Table IV describes the key findings and results of the study.

TABLE IV. KEY FINDINGS FROM THE DISRUPTION ANALYSIS OF THE MID-ATLANTIC INDUSTRIAL REGION.

Finding	Description
Disruption type impacts system orders	Sector-based disruptions produce stronger and sustained structural reordering relative to asset-based disruptions, even when fewer nodes are directly affected.
MMLPs buffer asset-layer cascades	The MMLP buffer reduces peak disruptiveness and accelerates recovery in asset-originated scenarios, but provides limited benefit when disruptions originate at the sector level and bypass asset-to-sector provision pathways.
Network connectivity and propagation	Scenarios targeting highly connected nodes (Communications, Emergency Services) produce widespread reordering, while scenarios targeting less connected nodes (Dams, Nuclear assets) remain localized.

These results support two broader observations. First, that operational capacity loss of and structural loss through disruption of system orders are complementary but distinct assessments of resilience. Two disruptions may result in similar capacity changes, but differ in how they reorganize system order of infrastructure components. Resilience assessments that rely on capacity alone may not address disruptions that alter system hierarchies. Second, results show that not all infrastructure investments provide uniform resilience benefits. The MMLP buffer is an example, where the additional capacity is effective when the disruptions are primarily to asset layers, but has reduced benefit if the disruption occurs in the abstract sectors. These observations drive the need for additional analytical methods that link infrastructure investments to improving predictable and trustworthy supply chains across different disruptive scenarios. Several limitations shape the scope of these results. Model parameters are based on subject matter expert elicitation rather than empirical calibration, and the asset inventory is representative rather than exhaustive. Future work will incorporate operational data, expand the asset inventory, and assess additional applications beyond freight and supply chains, including dams, agriculture, and water management systems.

REFERENCES

[1] Song, M., Ma, X., Zhao, X., and Zhang, L., "How to enhance supply chain resilience: A logistics approach," *The International Journal of Logistics Management*, vol. 33, no. 4, pp. 1408–1436, 2022,

[2] D.C. Loose, M.C. Marcellin, I. Linkov, G. Pavur, M. Kitsak, M.A. Deegan, and J. H. Lambert," Infrastructure network resilience analysis with disruptions of system order," *Proc. 11th 2025 International Conference on Control, Decision and Information Technologies (CoDIT)*, 2025.

[3] M. Rife, "Historic winter storm paralyzes the US; could cost over $100 billion," *Tampa Free Press / AOL News*, Jan. 25, 2026.

[4] R. M. Rinaldi, J. P. Peerenboom, and T. K. Kelly, "Identifying, understanding, and analyzing critical infrastructure interdependencies," *IEEE Control Systems Magazine*, vol. 21, no. 6, pp. 11–25, Dec. 2001.

[5] Q. Yang, C.M. Scoglio, and D.M. Gruenbacher, "Robustness of supply chain networks against underload cascading failures," *Physica A:Statistical Mechanics and its Applications*, vol. 563, 2021.

[6] M. Makaci, I. Zouaghi, P. Reaidy, K. E. Samuel, V. Botta-Genoulaz, and T.Monteiro, "Dynamic supply chain collaboration: A comprehensive typology for pooled warehouses," *The International Journal of Logistics Management*, vol. 36, no. 6, pp. 1709–1741, 2025.

[7] K. Klasa, B. D. Trump, S. Dulin, M. Smith, H. Jarman, and I. Linkov, "A resilience-augmented approach to compound threats and risk governance: A systems perspective on navigating complex crises," *Environments*, vol. 12, no. 2, p. 64, Feb. 2025, doi: 10.3390/environments12020064.

[8] Z. Arif, "Development of Logistics Parks in India; A step towards Supply Chain efficiency with less carbon" Siemens.com, 2025.

[9] D.C. Loose, M.E. Gunn, M.C. Marcellin, M.C. Gunn, F. Popoola, K.R. Jackson, E. Jehu, I. Linkov, and J.H. Lambert, "Enterprise resilience and trust in multiscale logistics systems," *in Proc. IEEE Int. Syst. Conf. (SysCon)*, Montreal, QC, Canada, 2026, in press.

[10] D. C. Loose, M. C. Marcellin, I. Linkov, G. Pavur, M. A. Kitsak, M. A. Deegan, and J. H. Lambert, "Order disruption and resilience of cyber-physical systems of a metropolitan region," *Proc. IEEE Int. Syst. Conf. (SysCon)*, 2025

[11] D.C. Loose, M.C. Marcellin, I. Linkov, G. Pavur, L.H. Hogewood, M.A. Deegan, and J.H. Lambert, "Stress testing of infrastructure networks and system order," in *Proc. IEEE Resilience Week (RWS)*, Dec. 2025.

[12] S. E. Galaitsi *et al.*, "Navigating the precipice: Lessons on collapse from the Late Bronze Age," *Risk Analysis*, vol. 45, pp. 2079–2082, 2025, doi: 10.1111/risa.70019.

[13] Cybersecurity and Infrastructure Security Agency (CISA), "Critical infrastructure sectors," U.S. Department of Homeland Security. [Online]. Available: https://www.cisa.gov/topics/critical-infrastructure-security-and-resilience/critical-infrastructure-sectors

[14] J. Jiang, Y. Chen, O. Lakhal, and R. Merzouki, "Event-triggered reconfiguration scheduling of hypergraph-based system-of-systems: The resilience reaction," in *Proc. IEEE Int. Syst. Conf. (SysCon)*, 2024, doi: 10.1109/SysCon61195.2024.10553514.

[15] S. Gong, Y. Ye, X. Gao, L. Chen, and T. Wang, "Empirical patterns of interdependencies among critical infrastructures in cascading disasters: Evidence from a comprehensive multi-case analysis," *Int. J. Disaster Risk Reduct.*, vol. 95, p. 103862, 2023, doi: 10.1016/j.ijdrr.2023.103862.

[16] T. Agryzkov, L. Tortosa, J. F. Vicent, and R. Wilson, "A centrality measure for urban networks based on the eigenvector centrality concept," *Environment and Planning B: Urban Analytics and City Science*, vol. 46, no. 4, 2019.

[17] B. Cetiner, E. Koc, L. Soibelman, E. Taciroglu, E.J. Lee, and A. Nutakki, "A granular simulation of bridge closures due to a southern California scenario earthquake and its effects on the disruption and recovery of freight traffic to and from ports of Los Angeles and Long Beach," in Proc. Amer. Soc. Civ. Eng. (ASCE) Int. Conf. Computing in Civil Eng., Los Angeles, CA, USA, 2019, pp. 575–585, doi: 10.1061/9780784482650.061.

[18] Ministry of Road Transport & Highways (MRTH), "Concept Note: Logistics Efficiency Enhancement Program (LEEP) Development of Multimodal Logistics Parks."

[19] B. D. Trump, S. E. Galaitsi, M. Kitsak, and I. Linkov, "Threat-agnostic resilience for critical infrastructure systems," *International Journal of Disaster Risk Reduction*, vol. 124, p. 105535, 2025.

a. Linkov, B. D. Trump, J. Trump, G. Pescaroli, W. Hynes, A. Mavrodieva, and A. Panda, "Resilience stress testing for critical infrastructure," *International Journal of Disaster Risk Reduction*, vol. 82, p. 103323, 2022.

[20] B. X. Dong, M. Shan, and B. G. Hwang, "Simulation of transportation infrastructures resilience: A comprehensive review," *Environmental Science and Pollution Research*, vol. 29, no. 9, pp. 12965–12983, 2022.

[21] N. K. Svendsen and S. D. Wolthusen, "Connectivity models of interdependency in mixed-type critical infrastructure networks," *Information Security Technical Report*, vol. 12, no. 1, pp. 44–55, 2007.

[22] G. Smith, "Identity and togetherness of systems," *Systems Engineering Body of Knowledge (SEBoK)*, v. 2.13, Nov. 2025. [Online]. Available: https://sebokwiki.org/wiki/Identity_and_Togetherness_of_Systems

[23] M. L. Hassler, D. J. Andrews, B. C. Ezell, T. L. Polmateer, and J. H. Lambert, "Multi-perspective scenario-based preferences in enterprise risk analysis of public safety wireless broadband network," *Reliability Engineering & System Safety*, vol. 197, p. 106775, 2020.

[24] P. Sedgwick, "Spearman's rank correlation coefficient," *BMJ*, vol. 349

[25] S. A. Modaberi, S. Tohidi, S. G. Zadeh, and T. G. Bolandi, "A review of power system resilience assessment and enhancement approaches by focusing on wind farms and wind turbines," *IET Renewable Power Generation*, vol. 17, no. 9, pp. 2391–2410, 2023.

[26] Virginia Chamber of Commerce, *Blueprint Virginia 2035: A Business Plan for the Commonwealth*. Richmond, VA, USA: 2025.

[27] Virginia Economic Development Partnership (VEDP), "Supply Chain Management," 2025. [Online]. Available: https://www.vedp.org/industry/supply-chain-management

[28] Bidgee, "*Mack Granite photographed in Australia*," Wikimedia Commons, Jun. 13, 2009. [Online]. Available: https://en.wikipedia.org/wiki/Mack_Trucks#/media/File:Mack_Granite_02.jpg

[29] focus_mankind, "Goods station and marshalling yard at Lucerne, Switzerland," Wikimedia Commons, 2003. [Online]. Available: https://commons.wikimedia.org/wiki/File:Rang_gueter_bahnhof_small.jpg